Spin populations in one-dimensional alternant spin systems: A theoretical approach

Bhargavi Srinivasan, Oliver Kahn, and S. Ramasesha

Citation: The Journal of Chemical Physics **109**, 5770 (1998); doi: 10.1063/1.477199
View online: http://dx.doi.org/10.1063/1.477199
View Table of Contents: http://scitation.aip.org/content/aip/journal/jcp/109/14?ver=pdfcov
Published by the AIP Publishing

Spin populations in one-dimensional alternant spin systems: A theoretical approach

Bhargavi Srinivasan and Oliver Kahn[a)]
Laboratoire des Sciences Moléculaires, Institut de Chimie de la Matière Condensée de Bordeaux, UPR CNRS No. 9048, 33608 Pessac, France

S. Ramasesha
Solid State and Structural Chemistry Unit, Indian Institute of Science, Bangalore 560 012, India

(Received 15 April 1998; accepted 9 July 1998)

Spin-density maps, deduced from polarized neutron diffraction experiments, for both the pair and chain compounds of the system $Mn^{2+}Cu^{2+}$ have been reported recently. These results have motivated us to investigate theoretically the spin populations in such alternant mixed-spin systems. In this paper, we report our studies on the one-dimensional ferrimagnetic systems $(S_A,S_B)_N$ where N is the number of AB pairs. We have considered all cases in which the spin S_A takes on allowed values in the range 1 to $\frac{7}{2}$ while the spin S_B is held fixed at $\frac{1}{2}$. The theoretical studies have been carried out on the isotropic Heisenberg model, using the density matrix renormalization group method. The effect of the magnitude of the larger spin S_A on the quantum fluctuations in both A and B sublattices has been studied as a function of the system size N. We have investigated systems with both periodic and open boundary conditions, the latter with a view to understanding end-of-chain effects. The spin populations have been followed as a function of temperature as well as an applied magnetic field. High-magnetic fields are found to lead to interesting re-entrant behavior. The ratio of spin populations $|P_A/P_B|$ is not sensitive to temperature at low temperatures. © *1998 American Institute of Physics.* [S0021-9606(98)70238-7]

I. INTRODUCTION

The synthesis and the study of thermodynamic properties of one-dimensional (1D) alternant spin systems represents one of the most original achievements of molecular magnetism. The first compound of this kind to be structurally characterized has the molecular formula $MnCu(dto)_2(H_2O)_3\cdot 4.5H_2O$ with dto = dithiooxalato.[1,2] The intrachain antiferromagnetic exchange interaction between unequal spins of the adjacent Mn^{2+} and Cu^{2+} ions makes the system an one-dimensional ferrimagnet. Indeed the $\chi_M T$ versus T (χ_M is the zero-field magnetic susceptibility per repeat unit and T the temperature) plot for this compound exhibits a rounded minimum, characteristic of the ferrimagnets. A whole family of one-dimensional ferrimagnets of the general formula $MCu(pba)(H_2O)_3\cdot 2H_2O$, where M^{2+} is a divalent transition metal ion of the first row, is now known. The generic structural motif of these systems consists of parallel, alternating bimetallic chains. Along the chain, M^{2+} and Cu^{2+} ions are bridged by oxamato ligands which possess a remarkable capability to transmit a strong antiferromagnetic superexchange interaction. The structure of one of these compounds with $M^{2+}=Mn^{2+}$ is shown in Fig. 1. The Mn^{2+} ion is in a distorted octahedral environment while the Cu^{2+} ion is in a square pyramidal coordination.

Most of the compounds in the above family, particularly $MnCu(pba)(H_2O)_3\cdot 2H_2O$ involving the $S_{Mn}=\frac{5}{2}$ and the $S_{Cu}=\frac{5}{2}$ spins,[3] have been extensively investigated, both from experimental and theoretical viewpoints. The synthesis of such quasi-one-dimensional[4] and quasi-two-dimensional[5] motifs, with a variety of transition metal ions has provided much impetus to experimental and theoretical studies in an already active field of research. Recently, the spin-density map for $MnCu(pba)(H_2O)_3\cdot 2H_2O$ was determined experimentally from polarized neutron diffraction. Theoretical spin-density maps have been obtained from density functional calculations[6] carried out on a single unit. Interestingly, similar studies have also been carried out on a compound whose structure consists of isolated $Mn^{2+}Cu^{2+}$ pairs[7,8] instead of $Mn^{2+}Cu^{2+}$ infinite chains. The experimental studies of the isolated pairs and the infinite chains has opened up the question of the evolution of spin densities as a function of system size. This question cannot be easily answered by the density functional theories, and the exact diagonalization (ED) methods along with the recent density-matrix renormalization group (DMRG) method appear to be the methods of choice.

Before we proceed to briefly describe the experimental results on the spin populations in these systems, we first clarify that the systems we study are electronic insulators. Consequently, the spin populations that we consider are not the local moments in itinerant systems, but refer to the local moments induced in a symmetry breaking external field. Thus, the experimental spin population on an atom in a molecular magnetic system represents the excess up-spin density on the atom when the system is under the influence of a strong magnetic field. The spin distribution studies in an AB bimetallic species, with S_A and S_B local spins, provide two

[a)]Electronic mail: kahn@icmcb.u-bordeaux.fr

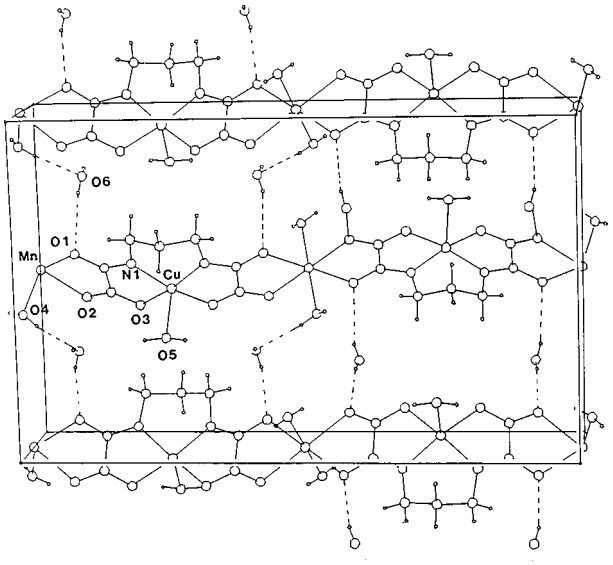

FIG. 1. Crystal structure of the compound $MnCu(pba)(H_2O)_3\cdot 2H_2O$ that provides a model system for an extended mixed spin chain.

kinds of information, namely: (i) The extent of spin delocalization (and spin polarization) from the A and B metal sites onto the nonmagnetic atoms in the structure, in particular those of the bridge; and (ii) the overall positive and negative spin populations at the A and B sites, defined as P_A and P_B, respectively. For example, in the case of $MnCu(pba)(H_2O)_3\cdot 2H_2O$, the spin-density maps show strong positive spin densities around the Mn^{2+} ion and weak negative spin densities around the Cu^{2+} ion. The delocalization of the spin density from the metal centers towards the oxamato bridging ligand is found to be more pronounced on the copper side than on the manganese side, so that the nodal surface (of zero spin density) is closer to manganese than to copper. The sum of the atomic spin populations on the manganese side (P_{Mn}) is found to be $5.05\ \mu_B$, and that of the negative spin populations on the copper side (P_{Cu}) is $-1.05\ \mu_B$.

The spin delocalization and polarization effects mainly depend on the nature of the A and B ions and the nature of the bridging and terminal ligands. To put it differently, they are related to the molecular details of the compound. On the other hand, the overall spin populations, P_A and P_B, besides depending upon the nature of A and B, also depend on the topology of the system. We could perhaps say that the spin populations on the nonmagnetic atoms are related to the chemistry of the system (bonding and superexchange pathways), while the overall P_A and P_B values are related to the physics of the system (effective exchange interactions). Our main concern in this paper are the total positive and negative spin populations, P_A and P_B, and not the details of the spin populations on the magnetic and nonmagnetic atoms.

This paper is devoted to a theoretical study of the spin populations in the alternant AB spin chains, with spins $1 \leqslant S_A \leqslant \frac{7}{2}$ and $S_B = \frac{1}{2}$. The spin S_B represents the Cu^{2+} ion and S_A represents other transition metal ions, depending upon the chosen value in the above range. In Sec. II we describe the ED and DMRG methods we have used. In Sec. III, we investigate the influence of the S_A value and the length of the $(AB)_N$ chain, defined as the number N of repeat units. We will also discuss end-of-chain effects by focusing on open boundary conditions. These studies are carried out as a function of both temperature and applied magnetic field.

II. COMPUTATIONAL SCHEMES

The Heisenberg Hamiltonian for a mixed spin chain of N units, with two spins S_A and S_B per unit cell is given by

$$\hat{H} = -J\sum_i \hat{S}_{Ai}\cdot\hat{S}_{Bi} + \hat{S}_{Bi}\cdot\hat{S}_{Ai+1}, \tag{1}$$

where $\hat{S}_A$ represents the larger spin, $\hat{S}_B$ the smaller spin, and J is the exchange constant, that is antiferromagnetic in the systems studied here. We introduce the notation $(S_A, S_B)_N$ for convenience. Thus, a spin 1–spin $\frac{1}{2}$ mixed spin system with N units would be represented as $(1,1/2)_N$.

We have studied the Hamiltonian in Eq. (1) using two techniques, namely, the exact diagonalization (ED) method and the recently developed density-matrix renormalization group (DMRG) method. In what follows, we describe briefly, for completeness, the implementation of the ED method and in greater detail that of the DMRG method.

A. The exact diagonalization method

The exact diagonalization method is used to obtain the model exact properties of a finite model spanning a finite dimensional Hilbert space. This is achieved by obtaining a matrix representation of the Hamiltonian in a convenient basis and using a numerical diagonalization algorithm to access either the full spectrum or a few low-lying eigenstates of the system. In our calculations, we employ the M_S basis to provide a matrix representation of the Hamiltonian. Thus for example, in the case of a $(1,\frac{1}{2})_2$ system, a possible state in the $M_S=0$ sector would be $|+1,+\frac{1}{2},-1,-\frac{1}{2},\rangle$, where the basis is described by the value of the spin projection at the m_S site. The basis states are generated as integers on the computer, using the states ''00,'' ''01,'' and ''10'' bit-states of two bits to represent the m_S value at each spin 1 site and ''1'' and ''0'' states of a single bit to represent the spin projections of the spin $\frac{1}{2}$ site. This representation of basis states by bits allows a unique association of a basis state with a $3N$ bit integer. For $2 \leqslant S_A \leqslant \frac{7}{2}$, each spin state of the $(AB)_N$ chain is represented similarly by a $4N$ bit integer.

The effect of single term in the Hamiltonian on a basis state is simply to alter the bit pattern of the state on which the term acts. The resulting integers represent another basis state and its ordinal number in the basis list provides the column index of the Hamiltonian matrix element to which the term contributes. The spin-angular momentum algebra provides the coefficient with which the new state would result. A few low-lying states of the Hamiltonian matrix obtained in a given M_S sector are computed using the Davidson algorithm.[9] When thermodynamical quantities like the magnetization are required, we need the full spectrum of the Hamiltonian matrix which is obtained by using standard mathematical libraries. This, however, places a severe re-

striction on the system size that can be studied; the largest matrix that we have diagonalized is of order 3400×3400.

B. The density matrix renormalization group method

The DMRG method, developed by White in 1992,[10,11] for interacting quantum lattice models such as the Hubbard and Heisenberg models, has proved to be very accurate in the study of 1D and quasi-1D systems. In the DMRG method, a systematic truncation of the Hilbert space is effected by resorting to the magnitude of the eigenvalues of the reduced density matrix as a criterion instead of the eigenvalues of the reduced Hamiltonian. Indeed, such a criterion was used by quantum chemists in studying the electron correlation problem. In the quantum chemical approach the eigenstates of the reduced one-body density matrix were employed as orbitals in Slater determinants, and only those eigenstates that corresponded to large eigenvalues of the reduced density matrix were retained. These eigenstates which came to be known as the ''natural orbitals'' were found to provide fast convergence in a configuration interaction scheme for correlation energies.

The scheme of White, although similar in spirit to the ''natural orbital'' approach, goes considerably beyond the earlier quantum chemical approaches by incorporating features of renormalization, that is retaining the order of the Hamiltonian matrix with increasing system size, even as the full dimensionality of the Fock space increases. Besides, the DMRG scheme of White deals with eigenvectors of the reduced many-body density matrices.

The DMRG algorithm for the $(1,\frac{1}{2})_N$ system proceeds along the lines described in an earlier study.[12] To briefly recapitulate, we first obtain all the eigenstates of a small system of $2n$ sites by exact diagonalization. The system is then assumed to be divided into two blocks of n sites each, the left (L) and the right (R) blocks. Any eigenstate of the $2n$ system can then be expressed in the direct product Fock space of the left and the right blocks. The reduced density matrix element ρ_{ij} of the block on the left in a given eigenstate is given by

$$\rho_{\alpha,ij}=\Sigma_k \phi_{\alpha,ik}\phi_{\alpha,jk}, \tag{2}$$

where α labels the eigenstate of the system and the remaining two indices on ϕ label the Fock-space basis of the left and the right parts, respectively.

The density matrices so obtained are diagonalized and a cutoff is imposed on the Fock-space dimensionality by retaining only m density matrix eigenvectors (DMEV) to span the spaces in each block. The m DMEVs retained correspond to the m highest eigenvalues of the density matrix. The left and right half-block Hamiltonian matrices H_L and H_R as well as other relevant site operators constructed in the Fock-space basis are transformed into the DMEV basis. In the process, we have also performed a renormalization of these block operators since the DMEV basis retained at this step does not span the full Fock space of the block. The Hamiltonian for the $2n+2$ site system is obtained by inserting two sites in between the left and right blocks. The matrix representation of this Hamiltonian is obtained in a product basis of the DMEVs of the left block, DMEVs of the right block and the Fock-space basis of the two added sites. This Hamiltonian is diagonalized and the desired eigenvector used to construct the density matrices of the left and right $n+1$ size systems, and the process described above is iterated. At each iteration of the DMRG scheme, all the necessary quantities such as site–spin densities and spin–spin correlation functions are computed. The algorithm described above is known as the infinite lattice algorithm. We have carried out the DMRG calculations using this algorithm, keeping up to 64 states of the density matrix, for open and periodic boundary conditions.

The DMRG method has been used very widely in recent years to study a variety of models like the Hubbard, Heisenberg and t-J models, and has been used to compute a wide variety of quantities, the Haldane gap being one of the first.[11]

III. RESULTS AND DISCUSSION

Our studies on the $(AB)_N$ systems are focused on the variation of site–spin populations as a function of chain length and the choice of boundary condition. This property is particularly relevant in the light of recent experimental studies.[6] Other properties such as low-lying excitations, spin correlations, effects of lattice distortions, as well as dependence of specific heat and magnetic susceptibility as a function of temperature have been extensively studied earlier by spin-wave theory (SWT), ED, and the DMRG methods,[12,13] for the general mixed spin chains.

A. Spin populations in mixed spin systems

The spin populations in mixed spin systems depend on various factors, namely the system size, the nature of boundary conditions and the type of substitution of the A site. The spin population at site X in the ith unit cell, defined as $g\langle S^e_{X,i}\rangle$, g being the Zeeman factor taken to be 2.0 in the following, provide a graphic description of some of the most important features of molecular magnetic systems, spin delocalization, and the presence of positive and negative spin densities that can be extracted from experiments.

The spin populations of mixed spin systems have been studied by polarized neutron diffraction (PND) and by density-functional theory (DFT), as discussed in Refs. 6 and 8. We have also carried out some calculations of spin populations in open-chain systems using the DMRG as presented in an earlier paper.[14] While these studies provide important insights into the nature and behavior of the $Mn^{2+}Cu^{2+}$ systems, there are many interesting questions to be addressed. The experimental quantities that we compare with are the integrated positive and negative spin populations, P_A and P_B, in the unit cell.

Earlier work on spin populations of the two $Mn^{2+}Cu^{2+}$ systems indicated important differences between the pair compound and the chain compound. The spin populations at the A and B sites of the pair compound can be calculated using simple spin coupling scheme to obtain the state $|2,2\rangle$ with $S=2$ and $M_S=2$, obtained from the spin states of the spin $\frac{5}{2}$ Mn^{2+} ion ($|S_{\mathrm{Mn}},M_{S,\mathrm{Mn}}\rangle$) and spin $\frac{1}{2}$ of the Cu^{2+} ion ($|S_{\mathrm{Cu}},M_{S,\mathrm{Cu}}$)

$$|2,2\rangle=(\tfrac{5}{6})^{1/2}|\tfrac{5}{2},\tfrac{5}{2}\rangle\cdot|\tfrac{1}{2},-\tfrac{1}{2}\rangle-(\tfrac{1}{6})^{1/2}|\tfrac{5}{2},\tfrac{3}{2}\rangle\cdot|\tfrac{1}{2},\tfrac{1}{2}\rangle, \tag{3}$$

which yields the values 4.67 and $-0.67\ \mu_B$ for the A and B sites. This is in remarkable agreement with the experimental spin populations P_A and P_B as estimated by PND, 4.67 and $-0.67\ \mu_B$ at the A and B sites.[8] Thus, this system is seen to be well described as an isotropic low-spin pair (Heitler–London) state. The theoretical study of the evolution to the solid state became necessary due to the synthesis of the chain compound and the subsequent polarized neutron diffraction study which showed the integrated spin densities in the chain to be 5.05 and $-1.05\ \mu_B$,[6] values very close to those of the Néel state. This seems to imply that the quantum fluctuations in the mixed spin chain are suppressed, a view that is contrary to the well recognized fact that the quantum fluctuations play an important role in low-dimensional systems.

This interesting experimental observation has necessitated an examination of the evolution of spin densities as a function of increasing chain length. We have examined the spin populations of mixed spin systems, for different chain lengths with both open and periodic boundary conditions, employing two different numerical techniques (ED and DMRG) as well as an analytical (SWT) technique. In comparing with experimental data, it is important to bear in mind that the neutron diffraction experiment probes the system at length scales of about 0.83 Å, where the Mn–Cu distances in these systems are between 5.2 and 5.4 Å. On the other hand, the theoretical values are obtained using a quantum lattice model which assumes spins to be localized at a lattice site. Thus, effects such as delocalization effects, seen very clearly in the experiment, cannot be obtained from this Hamiltonian. This is the reason for using the integrated positive and negative spin populations, instead of the bare populations at the Mn^{2+} and Cu^{2+} sites in the unit cell.

The SWT first introduced by Anderson[15] was extended to inorganic ferrimagnets as early as 1958[16] and more recently to the mixed spin molecular systems.[12,13,17] It is carried out using the Holstein–Primakoff transformation that maps a spin system on to a system of bosons. The bosonic Hamiltonian is truncated to bilinear order and diagonalized by a Bogoliubov rotation. From the resulting eigenstates, one obtains energy, sub-lattice magnetizations, spin–spin correlations, etc. We do not consider all of the above quantities as they have been studied elsewhere. Instead, we concentrate on the sub-lattice magnetization, which is in fact the spin population, except for a factor g. The sub-lattice magnetizations on the A and B sub-lattices of a mixed spin chain in the SWT scheme are given by[12,13]

$$\begin{aligned}\langle S_A^z\rangle&=\left(S_A+\frac{1}{2}\right)-\frac{1}{2}\int_0^\pi\frac{dk}{\pi}\frac{J(S_A+S_B)}{\omega_k},\\ \langle S_B^z\rangle&=S_B-S_A-\langle S_A^z\rangle,\\ \omega_k&=J\sqrt{(S_A-S_B)^2+4S_AS_B\sin^2\frac{k}{2}}.\end{aligned} \tag{4}$$

Thus, the effect of quantum fluctuations is seen to be the same for each sub-lattice and is given by

$$\Delta\langle S^z\rangle=\left(\frac{1}{2}\right)-\frac{1}{2}\int_0^\pi\frac{dk}{\pi}\frac{J(S_A+S_B)}{\omega_k}. \tag{5}$$

Since ω_k as a function of momentum, k, does not vanish linearly anywhere in the Brillouin zone, the above integral is well behaved. Consequently, there are no divergences in SWT for the mixed spin system. This situation should be contrasted with the pure spin $\frac{1}{2}$ Heisenberg antiferromagnet (HAFM) in one-dimension, where the correction to the sub-lattice magnetization due to quantum fluctuations is roughly given by $\int dk/k$.[18] This quantity diverges logarithmically, providing an indication that SWT is not a consistent description of the one-dimensional HAFM. In this respect, it should be noted that the mixed spin systems behave more like the Heisenberg ferromagnet than the antiferromagnet.

The DMRG data were obtained by imposing a cutoff of 50 in the DMRG procedure. Systems of up to 50 pairs were studied, with S_B fixed at $\frac{1}{2}$ and S_A taking values from 1 to $\frac{7}{2}$. We have shown the variation with system size only up to $N=12$, because the data already converges at this system size. Figure 2 shows the spin populations P_A for $S_A=1$ and $\frac{7}{2}$ on the A sites of closed mixed spin chains, as obtained from the DMRG calculations, against system size. These two S_A values are the smallest and the highest that we have considered, respectively. Data for $S_A=\frac{3}{2}$, 2, $\frac{5}{2}$, and 3 show qualitatively the same behavior but have not been displayed for clarity. In the lower graph of Fig. 2 we can see the spin populations P_B on the B sites of the mixed spin chains for four S_A values and different values of N. From Fig. 2, we see that the A and B sub-lattices of the mixed spin systems show very different behavior. The spin populations P_A converge much faster than the spin populations P_B. This is consistent with the view that the effect of quantum fluctuations is strongest at the spin $\frac{1}{2}$ sites. We also see from the figure that the spin populations P_A seem to converge better to their classical values, $2S_A$, than the spin populations P_B to their classical value of 1.0. In fact, the difference as the size of S_A is increased is striking, indicating that the system gets closer to a classical system as S_A increases. In Fig. 3 the ratio of the spin populations $|P_A/P_B|$ is plotted as a function of system size N for closed and open chains. From this we see that the convergence is faster in the closed system than in the open system, which is consistent with the observation that ground-state quantities tend to converge as $1/N^2$ for closed chains, and more slowly as $1/N$ for open chains. The spin populations converge to the same values for open and closed chains, as expected. However, the quantity plotted for open chains is the spin population at the middle of the chain. The spin population shows interesting variations along the length of the chain, and we next examine these end-of-chain effects.

In Table I the spin populations are presented at the A and B sites for systems with S_A ranging from 1 to $\frac{7}{2}$, for the pair, for the infinite system (that could be a ring or the middle sites of a chain) from the DMRG calculations and for the infinite system as obtained from SWT. It should be pointed out that the values from the DMRG correspond to the converged values obtained by increasing the system size. As already discussed, experimental data are available for the case $S_A=\frac{5}{2}$, and we see that the spin populations for the pair

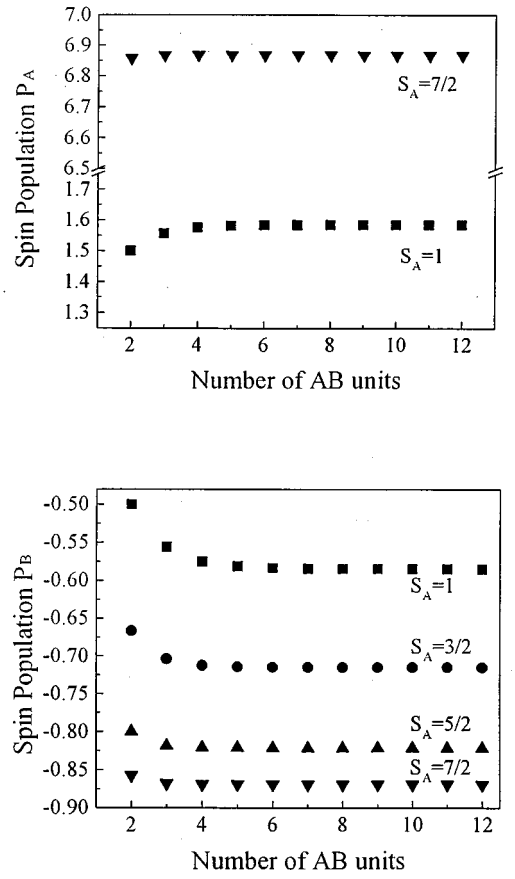

FIG. 2. (Top) Spin populations at the S_A sites vs system size N for closed chain mixed spin systems $(S_A,S_B)_N$, with S_A being 1 (squares) and $\frac{7}{2}$ (down-triangles); (bottom) Spin populations at the S_B (spin $\frac{1}{2}$) sites vs system size N for closed chain mixed spin systems $(S_A,S_B)_N$, with S_A being 1 (squares), $\frac{3}{2}$ (circles), $\frac{5}{2}$ (up-triangles), and $\frac{7}{2}$ (down-triangles).

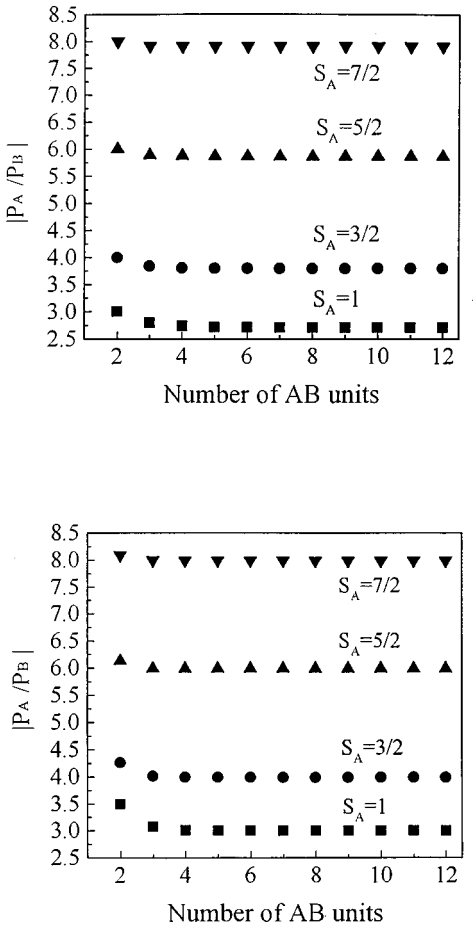

FIG. 3. (Top) Ratio of spin populations $|P_A/P_B|$ vs system size N for closed chain mixed spin systems $(S_A,S_B)_N$, with S_A being 1 (squares), $\frac{3}{2}$ (circles), $\frac{5}{2}$ (up-triangles), and $\frac{7}{2}$ (down-triangles); (bottom) Ratio of spin populations $|P_A/P_B|$ vs system size N for open chain mixed spin systems $(S_A,S_B)_N$, with S_A being 1 (squares), $\frac{3}{2}$ (circles), $\frac{5}{2}$ (up-triangles) and $\frac{7}{2}$ (down-triangles).

show remarkable agreement with the experimental values, 4.67 and $-0.67\ \mu_B$. In the case of the chain compound the experimental values are 5.05(7) and $-1.05(10)\ \mu_B$. The theoretical values of 4.82 and $-0.82\ \mu_B$ are in reasonable agreement with the experimental values, especially when one takes into account that length scales of about $\frac{1}{6}$ the lattice spacing are probed in the experiment, while the smallest length scale in the theory is the lattice spacing, by definition. It is also interesting to compare the values obtained from the DMRG with data from SWT, as shown in Table I. Interestingly, we notice that SWT overestimates quantum fluctuations in these systems. The SWT theory is in reasonably good agreement with the DMRG, especially as S_B becomes larger, indicating that SWT provides a physically consistent, if not exact description of these systems.

B. End-of-chain effects in open chains

In the preceding section, we dealt with the infinite system properties of mixed spin chains. For this reason, we dealt with properties of periodic chains or the properties of sites at the middle of open chains. However, experimental systems are not always infinite in extent and end-of-chain effects are often both observable and important. The finiteness of the system results in the environment of a spin in the middle of a chain being different from that at the ends. In fact, such effects have both been observed and studied, a notable example being the case of spin 1 Heisenberg chain. In this system it was predicted that there should exist two effective spin $\frac{1}{2}$-like objects at the end of the chain,[11] and in fact, evidence for this comes from the electron spin resonance (ESR) spectrum.[19]

Thus, in the mixed spin systems, we should expect to see differences in spin densities at sites in the interior of the system, compared to sites at the ends in the open chains. In Fig. 4, we present the spin populations P_A and P_B at each site of the $(1,\frac{1}{2})_6$ and $(1,\frac{1}{2})_{25}$ systems. We see that quite apart from the differences between the A and B sites, neither all the A sites nor all the B sites in all the unit cells are equivalent. Rather, there is a variation of the spin population at the A (B) sites along the chain. We notice that the spin populations are also not symmetrical about the middle of the chain, which is a direct consequence of the absence of reflection symmetry in an open $(S_A,S_B)_N$ chain. Thus, while the population at the A site is larger than its converged value at the left end of the chain, it is very small at the right end of the chain. The end-of-chain effects are qualitatively similar in the larger

TABLE I. Spin populations in units of μ_B for mixed spin systems $(S_A, S_B)_N$, with $S_B = \frac{1}{2}$. Data are for the pair system, obtained using the Clebsch–Gordan coefficients, the infinite system obtained using the DMRG and the infinite system, obtained from SWT.

	Pair		∞ chain (DMRG)		∞ chain (SWT)	
S_A	P_A	P_B	P_A	P_B	P_A	P_B
1.0	1.3333	−0.3333	1.5850	−0.5850	1.3902	−0.3902
1.5	2.5000	−0.5000	2.7152	−0.7152	2.6742	−0.6742
2.0	3.6000	−0.6000	3.7806	−0.7806	3.7298	−0.7298
2.5	4.6667	−0.6667	4.8212	−0.8212	4.7878	−0.7878
3.0	5.7142	−0.7142	5.8488	−0.8488	5.8252	−0.8252
3.5	6.7500	−0.7500	6.8690	−0.8690	6.8510	−0.8510

system. Thus, we see that end-of-chain effects are different from finite size effects. A qualitative picture of this behavior is provided in Fig. 5, where the lengths of the arrows indicate the magnitude of the spin population and the direction of the arrows, the sign. One can rationalize this phenomenon by representing each spin 1 as being two spin $\frac{1}{2}$ objects with a very strong ferromagnetic coupling. This would involve representing the spin 1 as the triplet state of two spin $\frac{1}{2}$ objects, obtained by projecting out other states. The antiferromagnetic coupling between the spin 1 and spin $\frac{1}{2}$ objects leaves an unpaired spin at one end while at the other we would be left with a paired spin. Such a microscopic description could provide a possible model for the end-of-chain effects seen in these systems.

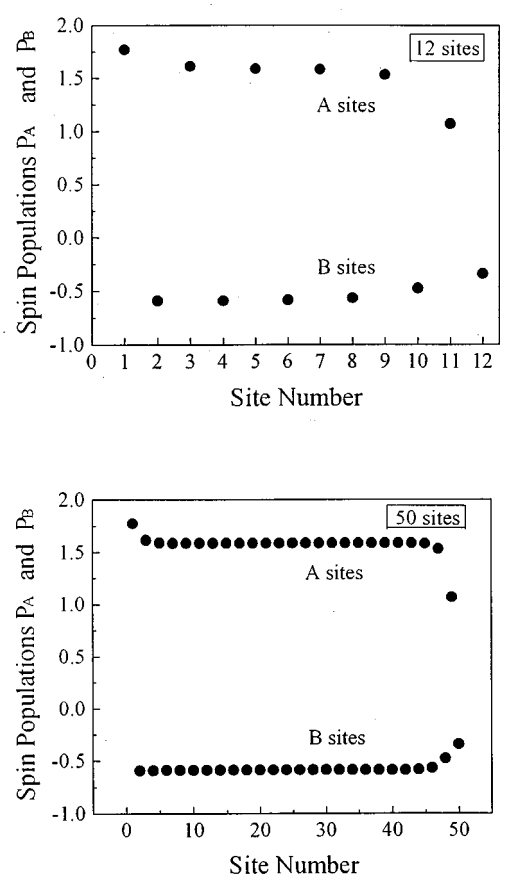

FIG. 4. Spin populations P_A and P_B vs site number for open chain mixed spin systems $(S_A, S_B)_6$ (top) and $(S_A, S_B)_{25}$ (bottom).

C. Effect of temperature

While we have so far discussed spin populations at $T = 0$ K, it is important to realize that experiments are carried out at finite albeit low temperatures, typically 4.2 K, in the presence of a strong magnetic field of about 5 T. We have, therefore, examined the effects of temperature in the presence of a magnetic field on the spin populations of these systems.

The temperature dependent spin populations are obtained from the standard expression

$$\frac{\Sigma_i \langle S_A^z \rangle \exp\left(\frac{-(E_i + BM_i)}{k_B T}\right)}{\Sigma_i \exp\left(\frac{-(E_i + BM_i)}{k_B T}\right)}, \tag{6}$$

where M_i is the z-component of the total spin in the state i with energy E_i and $\langle S_A^z \rangle_i$ is the spin population of the A site in the closed chain. Here, the magnetic-field B is in units of $|J|/g\mu_B$, and has the same units as energy. To get an idea of the field strengths, in these units, for an exchange parameter of 100 cm^{-1}, as in the $NiCu(pba)(H_2O)_3 \cdot 2H_2O$ compound,[3] $|J|/g\mu_B = 1.0$ would correspond to a magnetic field of 107 T and the experimental condition of 5 T would correspond to $\approx 0.05\,|J|/g\mu_B$. Calculating the temperature dependence of the spin populations at the A and B sites requires knowledge of the complete spectrum of the Hamiltonian. The results we

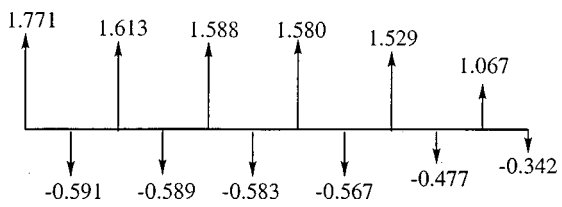

FIG. 5. Schematic representation of data presented in Fig. 4(a). Length of the arrow is proportional to the magnitude of the spin population and the direction corresponds to the sign. The spin populations are indicated at each site.

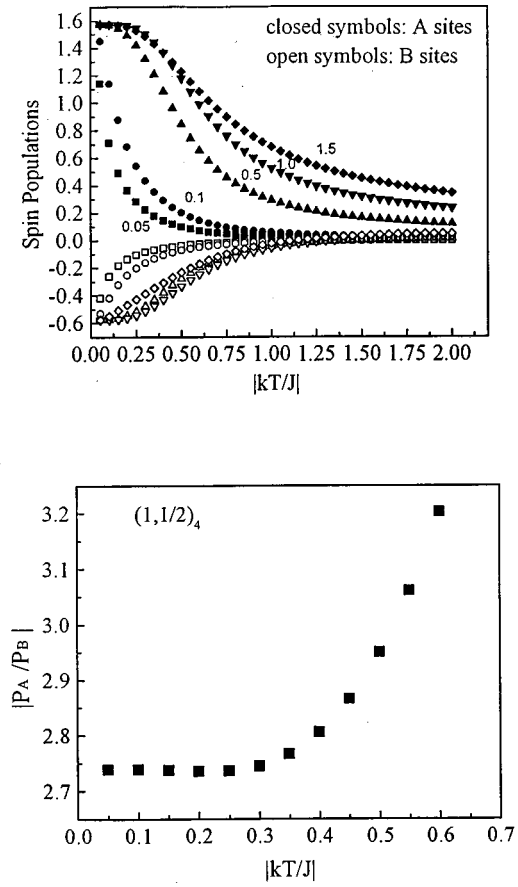

FIG. 6. (a) Variation of the spin populations at the A sites (closed symbols) and at the B sites (open symbols) for a $(1,\frac{1}{2})_4$ closed chain against $k_BT/|J|$ with field strength $B=0.05$ (squares), 0.1 (circles), 0.5 (up-triangles), 1.0 (down-triangles), and 1.5 (diamonds), in units of $|J|/g\mu_B$; (b) Ratio of spin populations $|P_A/P_B|$ vs system size $k_BT/|J|$ for the closed chain $(1,\frac{1}{2})_4$ system.

present here are for a $(1,\frac{1}{2})_4$ closed chain, which is the largest closed chain system accessible with the available computational resources, for ED studies.

In Fig. 6(a), we plot the variation of the spin populations at the A and B sites, in the presence of a magnetic field against temperature in units of $k_BT/|J|$. At low-magnetic fields and for small exchange constants ($B=0.05$ and $0.1\,|J|/g\mu_B$) the spin populations decay rapidly with increasing temperature and can be fitted to a sum of exponentials. In the high-temperature limit, the spin populations at both the A and the B sites are practically zero, which is the paramagnetic limit in which thermal fluctuations overwhelm any order imposed by the internal and external fields. Upon increasing the field strength to $B=0.5\,|J|/g\mu_B$, we observe that the spin populations no longer decay so rapidly at low temperature and instead show a plateau like behavior. This corresponds to the region in which $k_BT\approx|J|/g\mu_B$. This behavior is characteristic of the system, and we should expect to see this at lower magnetic fields for systems with smaller exchange constant.

Another very interesting feature of the spin populations is that increasing the magnetic field further leads to a reentrant behavior in the spin populations. This can be seen in the behavior of the spin populations at the B sites, where upon increasing the field from $0.05\,|J|/g\mu_B$ to $1.0\,|J|/g\mu_B$ leads to the plateau in spin populations discussed above. However, further increase in the field to $B=1.5\,|J|/g\mu_B$ results in the system regaining the low-magnetic field behavior; the plot for $B=1.5\,|J|/g\mu_B$ lies between those for $B=0.1\,|J|/g\mu_B$ and $B=0.5\,|J|/g\mu_B$. This behavior is consistent with the field dependent behavior of the magnetization obtained in an earlier study.[12] At very high fields, clearly, the external field dominates over any internal field in the material arising from exchange interactions. Thus, the temperature scale would no longer be set by J, the exchange parameter and would instead be set by the external magnetic field. The thermodynamics of such a system would be similar to that of a system of decoupled spins in a very strong magnetic field.

In Fig. 6(b) is shown the variation of the ratio $|P_A/P_B|$ against effective temperature $k_BT/|J|$ for the same system. Comparisons of the open and closed systems in Fig. 3 with experiments were based on zero temperature theory. From Figs. 6(a) and 6(b) we observe that while the actual spin populations seem to change very rapidly, even at low temperatures at a field of 5 T, the ratio $|P_A/P_B|$ is seen to change only gradually. It is important to keep in mind that the spin populations quoted from experiment are usually the normalized against the total spin population. Since the experiment is carried out in the presence of large but finite field, the spin populations obtained from experiment need to be rescaled to provide the expected saturation magnetization. Thus, the ratio of spin populations is a more relevant quantity for comparisons with experimental data. From Fig. 6(b) we see that the ratio $|P_A/P_B|$ shows a plateau like behavior up to $T\approx 0.3\,k_BT/|J|$ and rises very rapidly after. The temperature 4.2 K corresponds to about $0.007\,k_BT/|J|$ in this system. This value lies well within the plateau region in Fig. 6(b) and has a value of about 2.73. From Table I, the ratio at $T=0$ K is seen to have the value 2.71. Thus, the data shown in Fig. 6(b) serve to show that, in fact, data obtained at $T=4.2$ K are very close to the $T=0$ K values, provided that a normalization of the experimental spin populations is carried out.

IV. CONCLUSION

To summarize, the synthesis of mixed spin compounds in both pair and chain forms and subsequent polarized neutron diffraction studies motivated detailed theoretical studies on these systems. Our theoretical studies focus mainly on the analysis of spin populations, which have been obtained from the PND experiments in both the pair and the chain system. Our numerical calculations on Heisenberg models for mixed spin systems with both open and closed boundary conditions indicate remarkable agreement with experimental values for the pair and very good agreement with the values for the extended chain compound.

We have studied the evolution of the spin populations with system size, for both closed and open chains, and have also obtained values for the infinite system using the expressions from spin wave theory. Closed and open systems follow slightly different convergence paths, but converge even-

tually to the same values. The effect of quantum fluctuations is better seen in the S_B sub-lattice, as in the experiments. However, the size of spin S_A has a strong effect on the quantum fluctuations on the S_B sub-lattice, pushing the latter towards more classical behavior for larger S_A values. Open chains show interesting end-of-chain effects that have been studied. The effect of temperature and magnetic field on these systems has been explored. The field dependence is especially interesting and shows re-entrant behavior. A study of the ratio of spin populations $|P_A/P_B|$ serves to indicate that values obtained at the experimental conditions of 4.2 K and 5 T are very close to those at the absolute zero of temperature.

ACKNOWLEDGMENTS

We thank Swapan Pati and Diptiman Sen for many useful discussions and the Indo-French Centre for the Promotion of Advanced Research (IFCPAR) for partial support through grant No. G-1304 ''Chemistry and Physics of Molecular based materials.'' We also thank the Université de Bordeaux I and IDRIS, Orsay for computational facilities on the Cray YMP and the Cray computers, respectively.

[1] M. Verdaguer, A. Gleizes, and J. P. Renard, Phys. Rev. B **29**, 5144 (1989).
[2] A. Gleizes and M. Verdaguer, J. Am. Chem. Soc. **106**, 3727 (1984).
[3] Y. Pei, M. Verdaguer, O. Kahn, J. Sletten, and J. P. Renard, Inorg. Chem. **26**, 138 (1987).
[4] See for example, O. Kahn, *Molcular Magnetism* (VCH, New York, 1993).
[5] H. O. Stumpf, Y. Pei, O. Kahn, J. Sletten, and J. P. Renard, J. Am. Chem. Soc. **115**, 6738 (1993), J. Larionova, B. Mombelli, J. Sanchiz, and O. Kahn, Inorg. Chem. **37**, 679 (1998).
[6] V. Baron, B. Gillon, O. Plantevin, A. Cousson, C. Mathonière, O. Kahn, A. Grand, L. Ohrstrom, B. Delley, M. Bonnet, and J. X. Boucherle, J. Am. Chem. Soc. **119**, 3500 (1997).
[7] C. Mathonière, O. Kahn, J. C. Daran, H. Hilbig, and F. H. Kohler, Inorg. Chem. **32**, 4057 (1993).
[8] V. Baron, B. Gillon, O. Plantevin, A. Cousson, C. Mathonière, O. Kahn, A. Grand, L. Ohrstrom, and B. Delley, J. Am. Chem. Soc. **118**, 11822 (1996).
[9] E. R. Davidson, J. Comput. Phys. **17**, 87 (1975).
[10] S. R. White, Phys. Rev. Lett. **69**, 2863 (1992); Phys. Rev. B **48**, 10345 (1993).
[11] S. R. White and D. A. Huse, Phys. Rev. B **48**, 3844 (1993).
[12] Swapan K. Pati, S. Ramasesha, and Diptiman Sen, Phys. Rev. B **55**, 8894 (1997).
[13] Swapan K. Pati, S. Ramasesha, and Diptiman Sen, J. Phys.: Condens. Matter **9**, 8707 (1997).
[14] O. Kahn, C. Mathonière, Bhargavi Srinivasan, B. Gillon, V. Baron, A. Grand, L. Ohrstrom, and S. Ramasesha, New J. Chem. **21**, 1037 (1997).
[15] P. W. Anderson, Phys. Rev. B **86**, 694 (1952).
[16] J. Van Kranendock and J. H. Van Vleck, Rev. Mod. Phys. **30**, 1 (1958).
[17] S. Brehmer, H.-J. Mikeska, and S. Yamamoto, unpublished (preprint no. cond-mat V9610109).
[18] I. Affleck, J. Phys.: Condens. Matter **1**, 3047 (1989).
[19] G. E. Granroth, B. H. Ward, L.-K. Chou, S. Maegawa, N. S. Bell, J. H. Adair, D. R. Talham, and M. W. Meisel, unpublished (preprint no. cond-mat V9710161).